

5

PNe Extinction Determinations

5.1 Theory

Observed flux values are reduced from emitted flux values by interstellar extinction, which is a result of absorption and scattering of the radiation by dust in the ISM. This dust only makes up a small proportion of the ISM (~ 1 per cent by mass) but its effect can be considerable. Extinction is traditionally measured in magnitudes (which *decrease* with brightness), where a difference of 5 magnitudes corresponds to a brightness ratio of 100 to 1, i.e. $\Delta\text{mag} = 5$ corresponds to $\Delta\log_{10}f = 2$, which leads to the relationship between extinction, A , and a given flux ratio, F_R

$$A \text{ (mag)} = 2.5 \log_{10} F_R, \quad (5.1)$$

where $F_R = F_{\text{exp}}/F_{\text{obs}}$ is the expected to observed flux ratio, with fluxes normally measured in mW m^{-2} ($\text{erg cm}^{-2} \text{s}^{-1}$). It is this relationship that is the source of the ubiquitous factor of 2.5 seen in so many equations that relate extinction and flux.

As Fig. 5.1 shows, extinction varies inversely with wavelength, shorter wavelengths are more affected than longer wavelengths. Radio and infrared radiation pass through the ISM with ease, whereas optical starlight is reddened, since the extinction of blue light by dust is greater than that of red light. The degree of reddening is given in terms of the colour excess (in magnitudes), the difference between the observed and

5: PNE EXTINCTION DETERMINATIONS

intrinsic colour indices of a star:

$$E_{B-V} = (B - V) - (B - V)_0, \quad (5.2)$$

where $(B - V)$ and $(B - V)_0$ are the observed and intrinsic colour indices of the star, and B and V are the magnitudes measured with blue starlight (4400 Å) and greenish-yellow starlight (5500 Å) respectively. The colour index is the difference between the apparent magnitude of a star measured at one standard wavelength and another (longer) standard wavelength.

The ratio of total-to-selective extinction (or visual extinction to colour excess)

$$R = A_V/E_{B-V}, \quad (5.3)$$

compares the total extinction, typified by A_V , with the wavelength dependence of extinction as described by the colour excess, E_{B-V} . The value of R is found to depend on the size of dust grain responsible for the extinction. Fig. 5.1 shows the dependence of interstellar extinction, A_λ , on wavelength, λ , and for the visual part of the spectrum (3800–6800 Å), where the slope is fairly constant, $R_V = 3.1 \pm 0.1$ for typical regions of the ISM. According to Evans (1994), particles having $2\pi a/\lambda \simeq 1$, where a is the particle radius, provide the only means of giving rise to a λ^{-1} extinction law. The peak at 2175 Å corresponds to the high absorption of UV radiation by dust particles, which are in the small particle limit, i.e. they have radii $a \ll \lambda$, which for graphite means $a \leq 100$ Å (Whittet 1992). Where absorption occurs, the absorbed energy is re-emitted at much longer infrared wavelengths.

The extinction law can be normalised around the wavelength λ_V using

$$X = E_{\lambda-V}/E_{B-V}, \quad (5.4)$$

where X is usually plotted against λ^{-1} . In the limit, $X(\lambda \rightarrow \infty) = -R$, where the value of R can be read directly from the intercept of the ordinate axis. See Evans (1994) and Whittet (1992) for fuller treatments on the wavelength dependence of extinction.

The colour excess can also be expressed in terms of extinction values (in mag):

$$E_{B-V} = A_B - A_V, \quad (5.5)$$

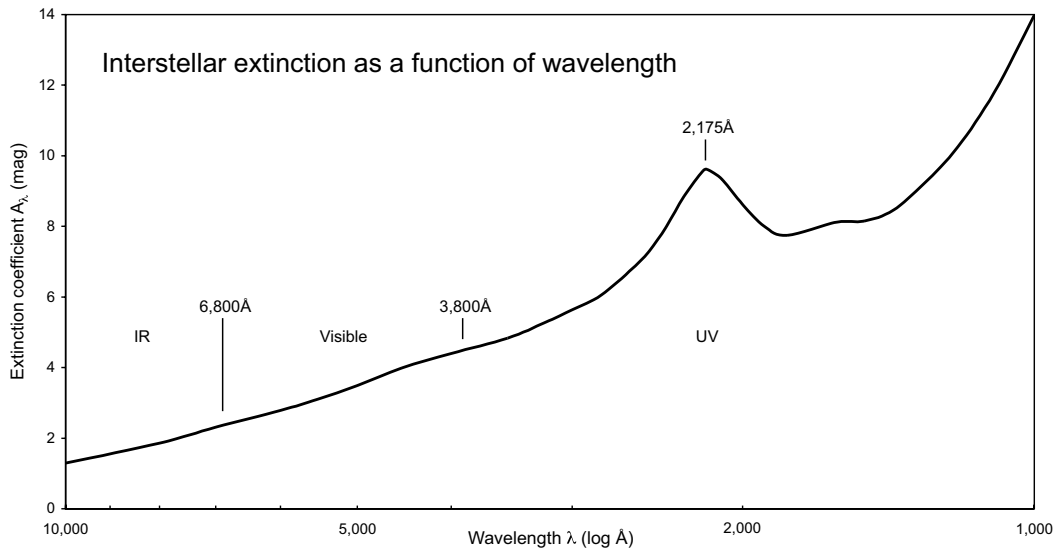


Figure 5.1: Interstellar extinction, A_λ (in magnitudes), as a function of wavelength, λ (\AA). The curve was obtained by a comparison of reddened and unreddened stars of the same spectral type (plotted from Pottasch 1984, p96, table 5.1).

where blue extinction, $A_B = B - B_0$, and visual extinction, $A_V = V - V_0$. Combining equations 5.1 and 5.5 gives an expression for colour excess in terms of flux ratios:

$$E_{B-V} = (A_B - A_V)/2.5. \quad (5.6)$$

As extinction varies with λ , an extinction coefficient, A_λ (in magnitudes), is introduced to provide an expression for extinction, C_λ , again in terms of flux ratios:

$$C_\lambda = A_\lambda(A_B - A_V)/2.5. \quad (5.7)$$

Fig. 5.1 plots the extinction coefficient, A_λ , of interstellar dust as a function of wavelength, λ (\AA), where the curve was obtained by a comparison of reddened and unreddened stars of the same spectral type. However, extinction in terms of flux is just the ratio of expected to observed flux values, and this flux ratio can be related to E_{B-V} using equations 5.5 and 5.7 and appropriate values for A_λ from Table 5.1:

$$C_\lambda = \log_{10} \frac{F(\lambda)_{\text{exp}}}{F(\lambda)_{\text{obs}}} = \frac{A_\lambda E_{B-V}}{2.5}. \quad (5.8)$$

Although the expected flux, $F(\lambda)_{\text{exp}}$, can not be measured directly, values can be determined from radio radiation, S_ν , which because of its much longer wavelength,

5: PNE EXTINCTION DETERMINATIONS

Table 5.1: Extinction coefficients, A_λ (magnitudes), for equation 5.8 (reproduced from Pottasch 1984, p96, table 5.1).

λ (Å)	A_λ	λ (Å)	A_λ	λ (Å)	A_λ	λ (Å)	A_λ
1100	11.80	1900	8.00	2500	7.29	4500	3.99
1200	10.25	2000	8.62	2600	6.81	5000	3.50
1300	9.22	2100	9.32	2800	6.06	5500	3.10
1400	8.46	2175	9.62	3000	5.64	6000	2.79
1500	8.15	2200	9.58	3200	5.28	7000	2.32
1600	8.12	2300	8.86	3500	4.84	8000	1.86
1800	7.75	2400	7.99	4000	4.40	10000	1.30

is not affected by extinction. Radio continuum emission and line emission are both proportional to the square of the nebula density, integrated over the volume:

$$S_\nu \propto \int^V \rho^2 dV \quad F(\lambda) \propto \int^V \rho^2 dV. \quad (5.9)$$

Therefore, the ratio of radio continuum to line emission is not dependent on density, although there is a small temperature dependence. With suitable parameters, it is possible to calculate the expected flux, $F(\lambda)_{\text{exp}}$, from observed radio emission, S_ν , and using observed flux, $F(\lambda)_{\text{obs}}$, values and equation 5.8, it is possible to calculate extinction, C_λ , in the line of sight to the PNe observed (Pottasch 1984, p92).

5.2 Method I

From the above and by comparing observed H α flux values with catalogued optical and radio fluxes, extinction values can be determined, and I now describe the methods used to arrive at my extinction values listed in Table 4.1 in section 4.2. From Pottasch (1984, p93, equation 4.26) the radio to H β flux ratio is

$$S_\nu / F(\text{H}\beta) = 2.51 \times 10^7 T_e^{0.53} \nu^{-0.1} Y \quad (\text{Jy/mW m}^{-2}), \quad (5.10)$$

where the H β flux is assumed to be optically thin, T_e is the electron temperature in K, ν is the radio frequency in GHz and Y is a factor incorporating the ionized He/H ratio:

$$Y = 1 + \frac{n(\text{He}^+)}{n(\text{H}^+)} + 3.7 \frac{n(\text{He}^{2+})}{n(\text{H}^+)}, \quad (5.11)$$

assuming $T_e \sim 1.4 \times 10^4$ K. The cosmic abundance of helium compared to hydrogen by number is ~ 6 per cent. So using reasonable values of $n(\text{He}^+)/n(\text{H}^+) = 0.045$ and $n(\text{He}^{2+})/n(\text{H}^+) = 0.015$, $Y = 1.1$. Setting $T_e = 10^4$ K, $\nu = 5$ GHz and converting to mJy gives

$$S_{\nu}(6\text{cm})/F(\text{H}\beta) = 3.10 \times 10^{12} \text{ (mJy/mW m}^{-2}\text{)}. \quad (5.12)$$

Using the first part of equation 5.8, H β extinction (C_β) can be defined as the ratio of expected to observed H β flux:

$$C_\beta = \log[F(\text{H}\beta)_0/F(\text{H}\beta)]. \quad (5.13)$$

As outlined in section 2.2, PNe are fully ionised, so if an electron density of $n_e = 10^4 \text{ cm}^{-3}$ is assumed, $T_e = 10^4$ K, and extinction is all external to the nebula, the Balmer-line intensity ratio, $F(\text{H}\alpha)/F(\text{H}\beta) = 2.85$ (Pottasch 1984, p41, table 3.1). Combining this factor with equations 5.12 and 5.13 gives an expression for H α extinction in terms of the observed (or catalogue) H α flux (mW m^{-2}) and the (catalogue) radio flux (mJy):

$$C_\alpha = \log[2.85S_{\nu}(6\text{cm})/3.10 \times 10^{12}F(\text{H}\alpha)]. \quad (5.14)$$

In order to compare observed *versus* catalogue extinction values, the latter can be derived from just the catalogue H α and H β flux values. I assume that the $F(\text{H}\alpha)/F(\text{H}\beta)$ ratio in the catalogue is accurate, even if the absolute fluxes are in doubt. I start with the full form of equation 5.13 (based on equation 5.8):

$$C_\beta = \log[F(\text{H}\beta)_0/F(\text{H}\beta)] = A_{4861}E_{B-V}/2.5 \quad (5.15)$$

where A_λ is the wavelength dependent extinction coefficient (listed in Table 5.1). It follows that

$$C_\alpha = \log[F(\text{H}\alpha)_0/F(\text{H}\alpha)] = A_{6561}E_{B-V}/2.5. \quad (5.16)$$

5: PNE EXTINCTION DETERMINATIONS

An expression for calculating $H\alpha$ extinction values in terms of catalogue $H\alpha$ and $H\beta$ flux values can now be derived. Rearranging and substituting equation 5.16 into the Balmer-line intensity ratio, $F(H\beta)_0 = F(H\alpha)_0/2.85$, gives:

$$F(H\beta)_0 = 10^{A_{6561}E_{B-V}/2.5} F(H\alpha)/2.85, \quad (5.17)$$

which when substituted into equation 5.15 gives:

$$\log[F(H\alpha)/2.85F(H\beta)] + A_{6561}E_{B-V}/2.5 = A_{4861}E_{B-V}/2.5, \quad (5.18)$$

and upon rearrangement gives an expression for the colour excess:

$$E_{B-V} = 2.5 \log[F(H\alpha)/2.85F(H\beta)]/(A_{4861} - A_{6561}). \quad (5.19)$$

All that remains is to substitute this expression for E_{B-V} into the latter part of equation 5.16 to get an expression for $H\alpha$ extinction, C_α , in terms of catalogue $H\alpha$ and $H\beta$ flux values:

$$C_{\alpha\text{opt}} = B \log[F(H\alpha)_{\text{cat}}/2.85F(H\beta)_{\text{cat}}], \quad (5.20)$$

where $B = A_{6561}/(A_{4861} - A_{6561}) = 2.28$ (using data from table 5.1, p96, Pottasch 1984).

5.3 Method II

An alternate method of calculating the wavelength dependent constant B in equation 5.20 is provided by Cardelli et al. (1989, hereafter CCM) in terms of what they consider a more fundamental extinction law A_λ/A_V , where A_λ is the absolute extinction at λ and A_V is the visual extinction. Based on empirical data, CCM provide a mean R_V [= A_V/E_{B-V}] extinction law, with wavelength dependent coefficients ($x = \lambda^{-1}\mu\text{m}^{-1}$), that takes the form

$$\langle A_\lambda/A_V \rangle = a(x) + b(x)/R_V, \quad (5.21)$$

where R_V is the ratio of visual extinction to colour excess. Dividing the expression for B by A_V and substituting the expression $a(x) + b(x)/R_V$ gives

$$B = \frac{(a_\alpha + b_\alpha/R_V)}{(a_\beta + b_\beta/R_V) - (a_\alpha + b_\alpha/R_V)}, \quad (5.22)$$

where $a_\alpha = a(1/\lambda_{H\alpha})$, $a_\beta = a(1/\lambda_{H\beta})$, etc.

Using the ‘standard’ value of $R_V = 3.1$ and appropriate values provided by CCM (equations 3a and 3b) for this polynomial in x gives $B = 2.36$, which is slightly higher than Pottasch’s value of 2.28. However, B is now dependent on the value of R_V so equation 5.20 takes the R_V dependent form:

$$C_{\alpha_{\text{opt}}} = B(R_V) \log[F(H\alpha)_{\text{cat}}/2.85F(H\beta)_{\text{cat}}]. \quad (5.23)$$

This enables R_V to be calculated in terms of the observed extinction C_α (equation 5.14) and catalogued $H\alpha$ and $H\beta$ flux ratios:

$$R_V = \frac{C_\alpha(b_\alpha - b_\beta) + Db_\alpha}{C_\alpha(a_\beta - a_\alpha) - Da_\alpha}. \quad (5.24)$$

where $D = \log[F(H\alpha)_{\text{cat}}/2.85F(H\beta)_{\text{cat}}]$.

5.4 Brightness temperature

The effect of high brightness temperature needs to be taken into account when using radio flux values to determine extinction. Brightness temperature is given by:

$$T_b = B_s \lambda^2 / 2k, \quad (5.25)$$

where λ is the observed wavelength, k is the Boltzmann constant and $B_s = S_\nu / \Delta\Omega$, is the surface brightness, i.e. flux density per unit solid angle. Substituting B_s and $\Delta\Omega = \theta^2 \pi / 4$ into equation 5.25 gives:

$$T_b = \frac{S_\nu 2\lambda^2}{\theta^2 \pi k} \quad (5.26)$$

in SI units. Setting $\lambda = 6\text{cm}$ and converting to mJy and arc seconds, I get an expression for brightness temperature, T_b , in terms of catalogue radio flux at 5 GHz and my observed angular diameters:

$$T_b = 70.62 S_{\nu, \text{line}} / \theta_{\text{line}}^2 \quad (\text{mJy} / \text{''}). \quad (5.27)$$

5: PNE EXTINCTION DETERMINATIONS

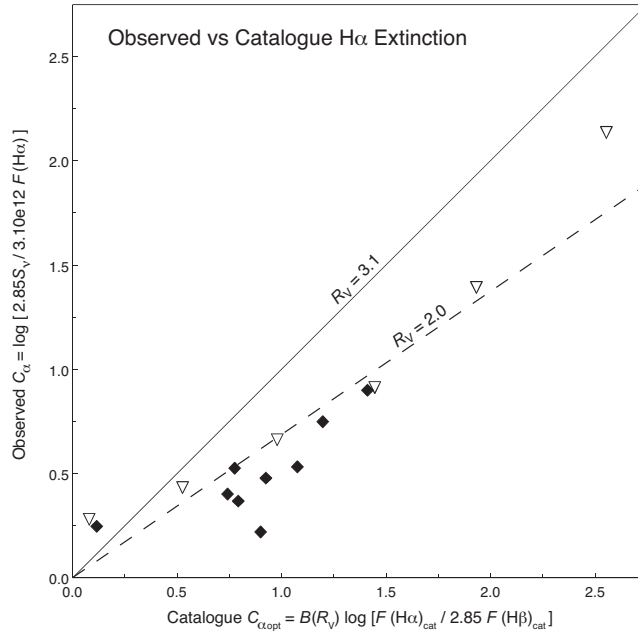


Figure 5.2: Comparison of observed $H\alpha$ extinction values (equation 5.14) and catalogued $H\alpha$ extinction values (equation 5.23) where $B(3.1) = 2.36$ for Bulge subset B objects. Diamonds denote objects observed on the first night, triangles the second.

For radio sources such as PNe, the brightness temperature may equal the physical temperature, if the nebula is optically thick, so for $T_b > 10^3$ K, the optical depth is likely to be high enough to make measured radio fluxes an underestimate of the true radio emission.

5.5 Results

My observed (equation 5.14) and catalogue (equation 5.20) extinction values are listed in columns nine and ten of Table 4.1. At high brightness temperatures, the optical depth of PNe reduces observed radio emission, so the observed extinction values are likely to be unreliable, as are those calculated from radio fluxes below 10 mJy (indicated in column 13). Therefore Fig. 5.2 only compares observed and catalogue extinction values for a subset of Bulge objects (hereafter subset B) with $100 \text{ mJy} > S_\nu > 10 \text{ mJy}$ and $T_b < 10^3$ K (equation 5.27). It can be seen that the values determined from my $H\alpha$

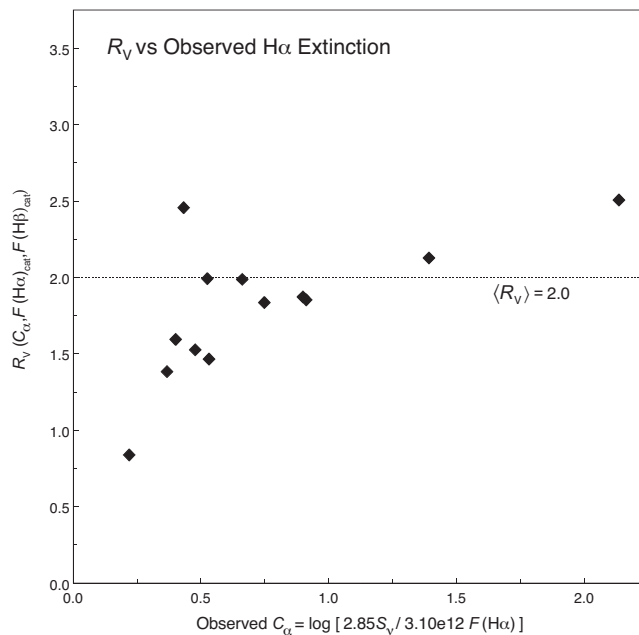


Figure 5.3: Comparison of R_V (equation 5.24) and observed $H\alpha$ extinction values (Bulge subset B). PN G 004.0–11.1 (M3-29) and 355.1–06.9 (M3-21) are excluded.

flux and catalogued radio flux tend to be lower than those calculated with $R_V = 3.1$ and catalogue $H\alpha$ and $H\beta$ fluxes. Subset B conforms to the Bulge criteria of Bensby and Lundström (2001) with the exception of 004.0–11.1 (M3-29) where $b = -11.1^\circ$ and 350.9+04.4 (H2-1) where $S_{5\text{GHz}} = 61$ mJy.

Calculated values for R_V (equation 5.24) are listed in column 11 of Table 4.1. Fig. 5.3 compares R_V with observed $H\alpha$ extinction values for subset B. The value of R_V is seen to be highly sensitive to differences between C_α and $C_{\alpha\text{opt}}$ with values > 10 for objects 004.0–11.1 (M3-29) and 355.1–06.9 (M3-21) not included in the figure for the sake of clarity (regardless of method, calculated extinction values for these two objects are very low with $\Delta F(H\alpha) = 0.1$, suggesting a possible error in the catalogue radio values). Apart from the value for 009.4–09.8 (M3-32) and the above two objects, there appears to be a correlation between increasing values of R_V and observed $H\alpha$ extinction.

Because of the sensitivity of R_V to differences between observed and catalogue extinction values, and the uncertainty in these values, a reasonable error, ΔR_V , has

5: PNE EXTINCTION DETERMINATIONS

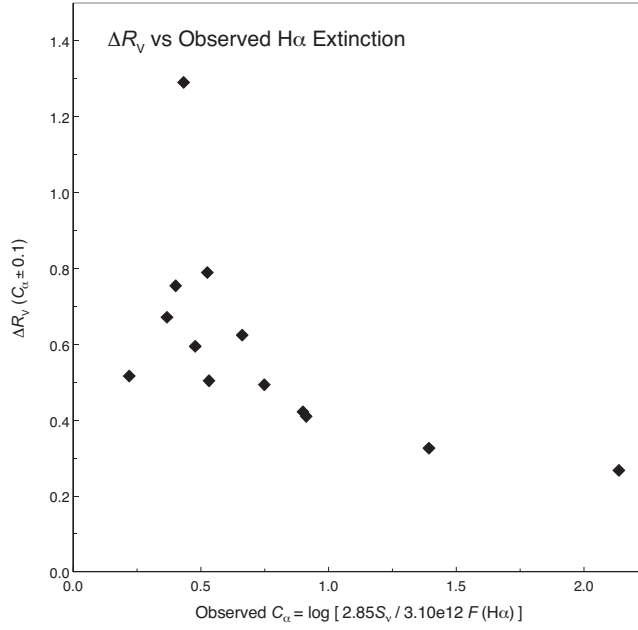


Figure 5.4: Comparison of ΔR_V (equation 5.28) and observed H α extinction values (equation 5.14) for Bulge subset B objects. PN G 004.0–11.1 (M3-29) and 355.1–06.9 (M3-21) are excluded.

been calculated with $C_\alpha \pm 0.1$ using

$$\Delta R_V = R_V(C_\alpha + 0.1) - R_V(C_\alpha - 0.1). \quad (5.28)$$

Using ΔR_V as the variance in R_V , the weighted mean value $\langle R_V \rangle$ is calculated using

$$\langle R_V \rangle = \frac{\sum R_V / \Delta R_V^2}{\sum \Delta R_V^{-2}}, \quad (5.29)$$

where each value for R_V in the sum is weighted inversely by its own variance ΔR_V (Bevington and Robinson 2003). For subset B, $\langle R_V \rangle$ is found to be 2.0 (indicated on Figs. 5.2 and 5.3). Values for ΔR_V are listed in column 12 of Table 4.1, and Fig. 5.4 compares ΔR_V with observed H α extinction values for subset B (except for 004.0–11.1 where $\Delta R_V \sim 6R_V$, and 355.1–06.9 where $\Delta R_V \sim 2R_V$).

For subset B a comparison of R_V with catalogue S_ν 6 cm radio values (Fig. 5.5) shows no evidence of a correlation between low values of R_V and low radio fluxes. In fact, radio flux values would have to increase by a factor ~ 3 in order for $\langle R_V \rangle \approx 3.1$.

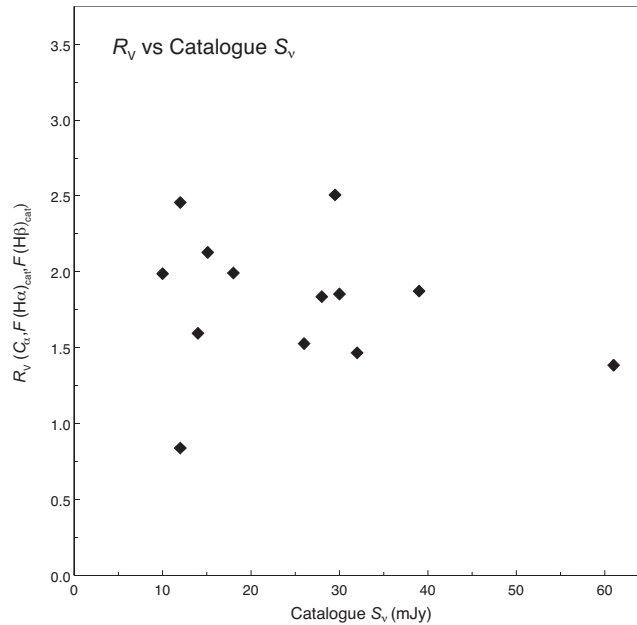


Figure 5.5: Comparison of observed R_V (equation 5.24) with catalogue S_V 6 cm radio values for subset B objects.

Fig. 5.6 compares R_V with Galactic distribution for subset B (again excluding 004.0–11.1 and 355.1–06.9). For the line of sight towards 351.1+04.8, the three objects close together on the sky (H2-1, M1-19 and M2-5) have, within their uncertainties, $\langle R_V \rangle = 1.2$. It is worth noting that the two Sagittarius dwarf galaxy objects 004.8–22.7 (He2-436) and 006.8–19.8 (Wray16-423) have $R_V = 3.1$ within their uncertainties.

Objects 352.6+00.1 (H1-12) and 352.8–00.2 (H1-13) have not been included in subset B because of their very high radio flux and being in the Galactic plane. Caswell and Haynes (1987) identify these positions with H II regions with $S_{5\text{GHz}}$ of 2.1 and 2.8 Jy respectively, giving higher values of R_V (2.4 and 3.5 respectively).

Values for $R_{V\text{cat}}$ and $\Delta R_{V\text{cat}}$ were also calculated using catalogue H α flux values in place of my observed values. The mean catalogue value $\langle R_{V\text{cat}} \rangle$ for subset B was found to be 2.2 and for the line of sight towards 351.1+04.8 it was 1.4. Fig. 5.7 compares observed and catalogue R_V values, and shows good agreement for subset B objects, apart from values for 009.4–09.8 (M3-32), 352.1+05.1 (M2-8) and 003.6+03.1 (M2-

5: PNE EXTINCTION DETERMINATIONS

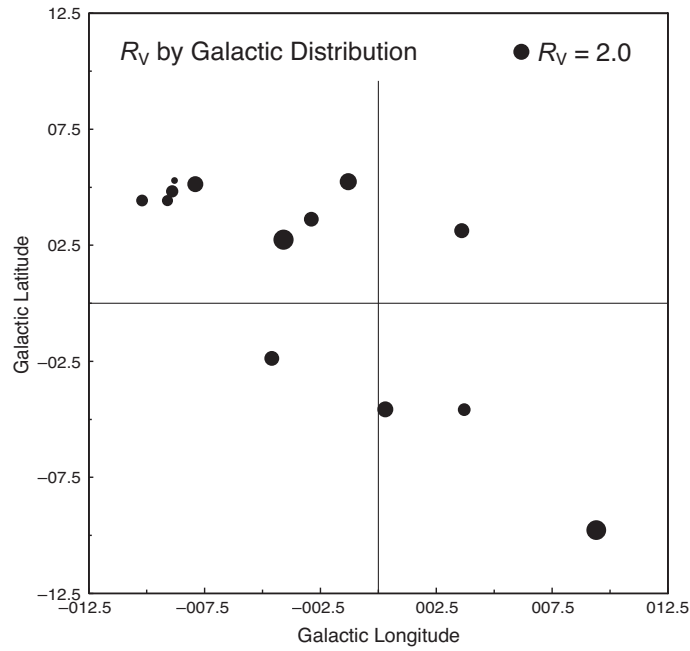


Figure 5.6: Comparison of R_V with Galactic distribution for Bulge subset B objects. Relative R_V is indicated by dot size with $R_V = 2.0$ scale indicated at top right. PN G 004.0–11.1 (M3-29) and 355.1–06.9 (M3-21) are excluded.

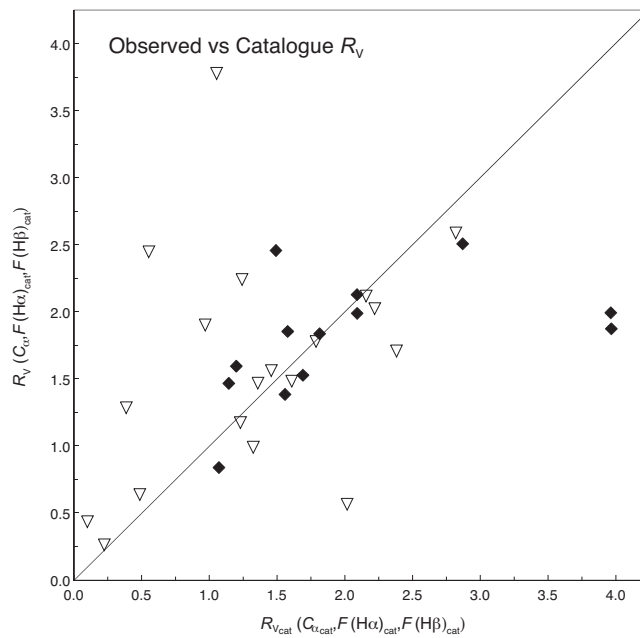


Figure 5.7: Comparison of R_V values (equation 5.24) calculated from observed and catalogue $H\alpha$ extinction. Diamonds denote Bulge subset B objects.

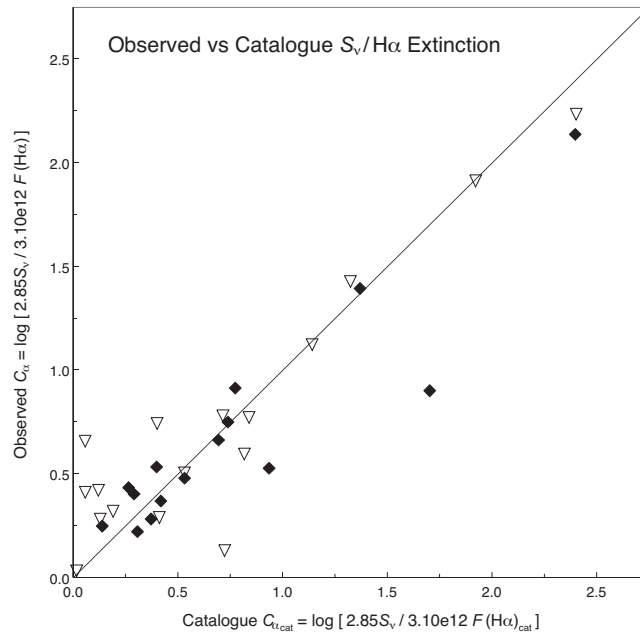


Figure 5.8: Comparison of $H\alpha$ extinction values derived from observed and catalogue $S_v/H\alpha$ ratios (equation 5.14) for Bulge subset B objects.

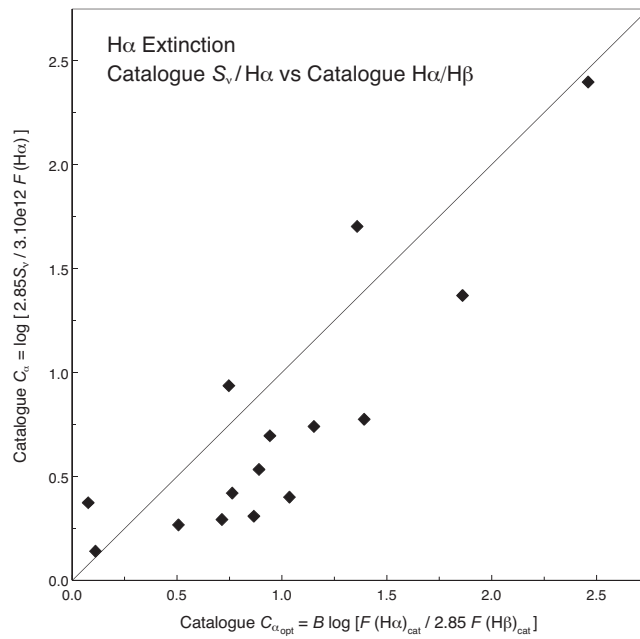


Figure 5.9: Comparison of $H\alpha$ extinction values derived from catalogue $S_v/H\alpha$ ratios (equation 5.14) and catalogue $H\alpha/H\beta$ ratios (equation 5.20) for Bulge subset B objects.

5: PNE EXTINCTION DETERMINATIONS

14). This suggests that in addition to my newly observed $H\alpha$ flux values, existing catalogue flux values also predict that interstellar extinction toward the Bulge is lower than that corresponding to the standard extinction curve $R_V = 3.1$.

Fig. 5.8 compares observed and catalogue $S_V/H\alpha$ extinction values (equation 5.14) and also shows good agreement for subset B, apart from values for 352.1+05.1 (M2-8) and 003.6+03.1 (M2-14), which have differences between observed and catalogued $H\alpha$ flux values, $\Delta F(H\alpha)$ of 0.4 and 0.8 respectively. Excluding the above three objects from subset B has no effect on the calculated values of $\langle R_V \rangle$ and $\langle R_{V\text{cat}} \rangle$. There was no evidence for systematic differences due to time of observation or position in the sky for these three objects. Finally, Fig. 5.9 compares $H\alpha$ extinction values derived from catalogue $S_V/H\alpha$ ratios (equation 5.14) and catalogue $H\alpha/H\beta$ ratios (equation 5.20), confirming that, for Bulge subset B objects, extinction values based on catalogue $H\alpha/H\beta$ ratios tend to be higher than those calculated from $S_V/H\alpha$ ratios.